

## Comparison of cure characteristics and mechanical properties of nano and micro silica-filled CSM elastomers

Tahereh Alsadat Tabaei, Rouhollah Bagheri, Mahdis Hesami

Chemical Engineering Department, Polymer Group, Isfahan University of Technology, Isfahan, Iran 84156

Correspondence to: M. Hesami (E-mail: mahdishesami@gmail.com)

**ABSTRACT:** In this study, the effect of micro and nano silica and their combination on mechanical and thermal properties of Chloro-sulfonated Polyethylene compounds were investigated. Cure characteristics were studied using a Monsanto Moving Die Rheometer at 155°C. Incorporation of nano silica accelerated the vulcanization whereas the micro silica particles decelerated the curing process. Both micro and nano silica increased the crosslink density as evidenced by swelling test. However, this value has been more improved in CSM/nano silica composites. The physico-mechanical properties of CSM/nano silica are superior compared to CSM/micro silica. Nano silica provided reinforcing efficiency which is not only because of higher specific surface area but also because of various interactions and especially physical interactions which are discussed in the text. Nano silica particles also improved the thermal properties more efficiently. Incorporation of 15 phr (part per hundred) nano and 5 phr micro silica to polymer improved the initial decomposition temperature for about 51°C and 16°C, respectively, using a TGA. The combination of micro and nano silica, showed that by coupling nano and micro fillers, the loading of fillers can be minimized. In other words, the hybrid samples with a lower filler loading behave as efficient as their separate counterpart with higher loading. © 2015 Wiley Periodicals, Inc. *J. Appl. Polym. Sci.* **2015**, *132*, 42668.

**KEYWORDS:** crosslinking; elastomers; mechanical properties; rubber; thermogravimetric analysis

Received 20 March 2015; accepted 26 June 2015

DOI: 10.1002/app.42668

### INTRODUCTION

Polymer-inorganic composites are of strong technological importance and extensively used in the industry. Nevertheless, many aspects on the structure-properties relations in these composites are still not well understood. Silica is one of the widely used reinforcing fillers especially for light-colored rubber products. The surface of hydrated silica is highly polar and hydrophilic because of the presence of numerous silanol groups.<sup>1</sup> This characteristic is a two-sided sword, the silanol groups have advantages as well as disadvantages. They cause silica-rubber interaction and can even form primary chemical bonds with functionalized polymers. Although the presence of silica has negative effects on cure because the silanol groups on silica surface could adsorb the cure activator necessary for sulfur vulcanization,<sup>2-4</sup> resulting in the delay of vulcanization.<sup>5-7</sup> The silanol groups on the surface of silica also enhance the filler-filler interaction and cause a difficulty in the dispersion of filler in the matrix. The reinforcement of an elastomer by a filler such as silica is not only associated with properties of polymer matrix and filler, it also depends on concentration of other components, particle shape and size, surface area, concentration of functional groups present on the surface of filler and degree of dispersion and distribution of filler. As compared to micron

size filler particles, nano size fillers are able to occupy substantially greater number of sites which provide reinforcing efficiency.<sup>8</sup> The crosslink density and mechanical properties are also influenced by structure and surface chemistry of nano silica.

Silica nano particles are also good choice for rubber industry especially for light colored products. The interaction between silica and rubber and its effect on properties of rubber have been studied extensively. It is confirmed that functionalized polymers such as chlorosulfonated polyethylene (CSM), can form primary chemical bonds with silica.<sup>6</sup> Also a great affinity towards polar sites on silica surface and rubbers such as CSM, CR, NBR has been reported.<sup>9-11</sup> Roychoudhury *et al.* studied the interaction between silica nano particles and CSM rubber.<sup>11</sup> Such interaction is due to the presence of silanol groups on the silica surface and sulfanyl chloride groups of CSM.

The preparation of rubbers filled with nano-and micro-silica fillers has already been reported by several researchers.<sup>12,13</sup> They claimed that the most important issue in nanocomposite preparation is the dispersion of nanofillers in the matrix. In order to improve dispersion and interfacial interaction between silica and CSM, Bai *et al.* functionalized the silica nano particles with CSM molecular chains.<sup>13</sup> For this purpose, they used in situ

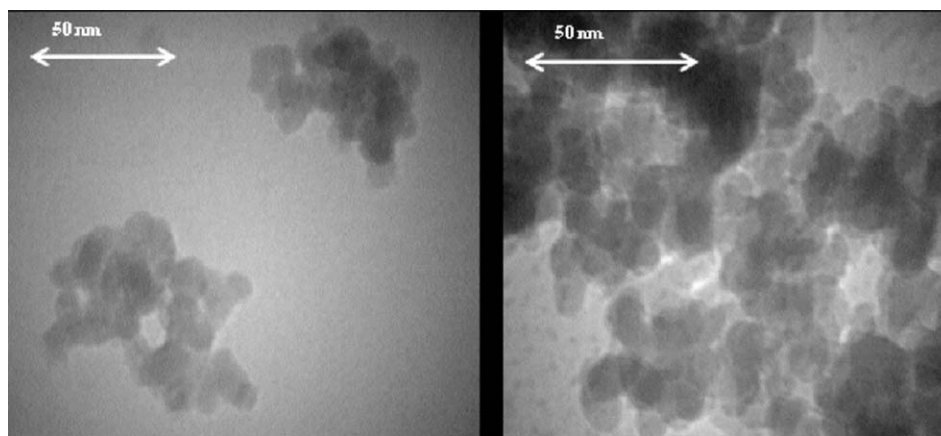


**Figure 1.** TEM micrograph of the used silica nano particles.

ultrasonication method which causes the reaction between silanol groups of silica and chlorine groups of CSM. They concluded that by using this method the mechanical properties, thermal stability and rheological properties of the nanocomposites were improved. Although functionalization of nano fillers will result in a good dispersion state, it is not cost-effective especially for industrial application.

Although, there are few research works dealing with CSM rubber and especially its nanocomposite,<sup>9,10,14–16</sup> the effect of some fillers such as carbon black<sup>10</sup> and nano clays<sup>9</sup> on physico-mechanical and electrical properties of CSM vulcanizates has been studied. The systematic study of the CSM rubber filled with nano- and micro-silica particles has not received much attention till now.<sup>12</sup> Because of the exceptional properties of CSM and its applicability for special purposes it is desired to study its properties. CSM as a component of polymer blends has been studied extensively, but in some applications it is necessary to use it alone. The literature have almost exclusively focused on blends of CSM and there are rare reports on CSM rubbers alone.<sup>13,14</sup> Since this rubber possesses good electrical, weather and chemical properties, in some application such as nuclear plant cable sheath it should be used alone.<sup>17</sup> Because of the excellence of melt blending method in nanocomposite preparation, this method has been applied in this work. In this work, the effect of nano- and micro-silica particles on the mechanical properties, cure characteristics and thermal stability of rubber matrix based on Chlorosulfonated Polyethylene rubber have been studied. To evaluate the dispersion state, the fracture surface of the crosslinked rubbers was observed by scanning electron microscope (SEM). The crosslink density of the rubber samples was also determined by swelling measurement. At the end of the article, the impact of both nano and micro silica fillers is studied in order to introduce a proper sample for industrial applications.

## EXPERIMENTAL

### Materials

Chlorosulfonated polyethylene rubber, CSM, (Hypalon 40), ( $\rho = 1.18 \text{ g/cm}^3$ ,  $M_w = 5.52 \times 10^5$ ,  $M_w/M_n = 1.97$ ), with 35% chlorine and 1% sulfur by weight, Mooney viscosity 56 (ML1+4 at 100°C), manufactured by DuPont, was used. The

fillers used in this study were: active precipitated nano-silica particles (BET 200–240  $\text{m}^2/\text{g}$ ,  $\rho = 50 \text{ g/L}$ , pH = 5–6, with the average size of 20–25 nm) and micro-silica particles (BET: 56–96  $\text{m}^2/\text{g}$ , pH 7.8 with the average size of 1.2  $\mu\text{m}$ ) were supplied by Fadak, Iran. Figure 1 shows the TEM micrograph of the used silica nano particles. The curing system includes the following materials: stearic acid was obtained from Merck, Germany, magnesium oxide (MgO), tetra methyl thiuram disulfide (TMTD), and 2-mercaptobenzothiazol (MBT) were supplied by Lanxess, Germany, sulfur ( $\text{S}_8$ ) was supplied by Tesdak, Iran.

### Sample Preparation

Table I shows the ingredients in two series of micro (M) and nano (N) formulations. The letters (M, N) are followed by numbers (5, 10, 15, 20) indicating concentration of the particles in the samples. The mixing of components was carried out in a two roll mixing mill (325 mm  $\times$  150 mm) having a friction ratio of 1 : 1.2, at a roller temperature of  $40 \pm 5^\circ\text{C}$ . The nip gap was 0.8 mm and the mixing time was 20 min, with careful control of uniform cutting operation. Two series of Chlorosulfonated Polyethylene compounds were prepared using a base formulation.<sup>2,10</sup> The preferred compounds were conditioned at room temperature for 24 h before cure. The vulcanization of all specimens was carried out in an electrically heated laboratory hydraulic press under a pressure of 15 MPa at 155°C (platen size: 300  $\times$  300 mm) by considering the optimum cure time ( $t_{c90}$ : 90% of the maximum cure). Cure characteristics were studied using a Monsanto Moving Die Rheometer at 155°C according to ASTM D5289-95.

### Methods of Characterization

**Rheometric Characteristic.** The cure characteristics, i.e.,  $M_L$  (minimum torque),  $M_H$  (maximum torque),  $t_{c90}$  (optimum cure time),  $t_{s2}$  (scorch time: time to 2 units of torque increase above minimum torque) and CRI [cure rate index is given by eq. (1)] of CSM compounds were determined by Monsanto Moving Die Rheometer at 155°C according to ASTM D 5289-95. It is reported earlier that the torque difference ( $M_H - M_L$ ) is directly proportional to the degree of crosslinking of the vulcanizates.<sup>18</sup> Furthermore it has been proposed that, to evaluate the reinforcing potential of the filler of the samples the  $\alpha_f$  value, given by eq. (2) is used.<sup>19</sup>

**Table I.** Formulations of Nano/Micro-Silica Filled CSM Compounds (phr)

Component, phr	Sample code								
	Control	M5	M10	M15	M20	N5	N10	N15	N20
CSM	100	100	100	100	100	100	100	100	100
Micro-silica (M)	0	5	10	15	20	0	0	0	0
Nano-silica (N)	0	0	0	0	0	5	10	15	20
Stearic acid	2	2	2	2	2	2	2	2	2
MgO	5	5	5	5	5	5	5	5	5
TMTD	2	2	2	2	2	2	2	2	2
MBT	1	1	1	1	1	1	1	1	1
S <sub>8</sub>	1.25	1.25	1.25	1.25	1.25	1.25	1.25	1.25	1.25

<sup>a</sup>phr: parts per hundred rubber.

$$\text{CRI} = \frac{100}{(t_{c90} - t_{s2})} \quad (1)$$

$$\alpha_f = \frac{\left(\frac{\Delta M_f}{\Delta M_g} - 1\right)}{w} \quad (2)$$

where  $\Delta M_f$  and  $\Delta M_g$  denote the torque difference ( $M_{\max} - M_{\min}$ ) during vulcanization for the filled and unfilled rubber, respectively, and “ $w$ ” represent the weigh fraction of the filler in the compound.

**Solvent Swelling Study and Cross-Linking Density Determination.** The cross-link density defined as the number of effective network chains per unit volume of rubber is denoted as  $\mu$ . This parameter was measured on the basis of the rapid solvent-swelling measurements by immersing the samples in 100 mL toluene to attain equilibrium swelling. The samples were allowed to swell for 72 h at 25°C, then they were taken out from toluene. The solvent was blotted from the surface of the samples and weighed immediately. The chemical cross-link density was calculated by the Flory–Rehner equation eq. (3).<sup>20</sup>

$$\mu = \frac{-[\ln(1-v) + v + \chi v^2]}{V \left[ v^{1/3} - \frac{v}{2} \right]} \quad (3)$$

where  $\chi$  is the polymer-solvent interaction parameter (Flory-Huggins's interaction parameter), which was found to be 0.401,<sup>20</sup>  $v$  is The volume fraction of rubber and  $V$  is the molar volume of the solvent (106.3 cm<sup>3</sup>/mol).<sup>21</sup> The volume fraction of rubber ( $v$ ) in the vulcanizates was determined by equilibrium swelling in toluene, using the method reported by Markovic *et al.* using eq. (4).<sup>13</sup>

$$v = \frac{1}{1 + \left\{ \frac{m_s - m_{ex}}{m_{ex}} \right\} \left\{ \frac{\rho_p}{\rho_s} \right\}} \quad (4)$$

where  $v$  is the volume fraction of the polymer in the swollen gel;  $m_s$  and  $m_{ex}$  are the weights of the specimen after and before swelling respectively;  $\rho_p$  and  $\rho_s$  are the density of rubber and solvent, respectively.

**Mechanical Testing.** The tensile properties of the vulcanizates such as tensile strength, elongation at break, and modulus at 100% extension (M100), 200% (M200), and 300% (M300) were

determined using a universal testing machine (Hoshmand HTSM 201). The dumbbell shaped specimens were punched from a 2 mm thick molded rubber sheet according to ASTM D-412. Tensile test was performed at room temperature with a crosshead speed of 50 mm/min. At least three samples were tested and the average values were calculated.

**Hardness Measurement.** The hardness of the samples was determined using Shore A type indentation hardness tester (Hiwa 500) according to DIN-53505. Five specimens test were examined for the test. The samples with a thickness of 8 mm were used for this test.

**Compression Set.** To evaluate the compression set of the samples, a cylindrical shaped sample has been compressed to 25% of its original thickness. The compressed sample was held between the plates of the compression set device, for 22 hours at 100°C according to ISO815-1991.

**Abrasion Resistance.** Abrasion loss of the samples was measured using a Hiwa 700 abrader according to DIN53-516. The cylindrical shaped samples were used for this test and the values were reported in cubic centimeter per hour (cm<sup>3</sup>/h) which is the volume in cm<sup>3</sup> abraded from a test piece per 40 meter. The abrasion resistance of a solid body is defined as its ability to withstand the progressive removal of the material from its surface, as the result of mechanical action of an erosive nature. The values reported are based on averages of three measurements for each sample.

**Scanning Electron Microscopy (SEM).** The scanning electron microscopy images of the fractured surfaces of the tensile-tested specimens were taken using a S-4160, Hitachi, Osaka, Japan; Acceleration voltage: 15 kV. The samples were sputter-coated with a thin layer of gold. The aim was to study the morphology of the samples and to evaluate the dispersion of the fillers in the polymer matrix.

**Thermo Gravimetric Analysis (TGA).** The thermal stability of the samples (unfilled and filled vulcanizates) was investigated by non-isothermal thermo gravimetric analysis using a Rheometric scientific. The measurements were conducted at heating rate of 10°C/min in a dynamic nitrogen atmosphere, in the

**Table II.** The Cure Characteristics of Nano- and Micro-Silica Particles Sized Filled CSM Vulcanizates

Cure characteristics	Sample code								
	Control	M5	M10	M15	M20	N5	N10	N15	N20
$M_L$ (dN.m)	0.72	0.72	0.72	0.72	0.79	0.65	0.79	1.08	2.58
$M_H$ (dN.m)	5.39	6.18	6.68	7.27	7.76	6.46	7.9	10.63	15.6
$\Delta M$ (dN.m)	4.67	5.46	5.96	6.55	6.97	5.81	7.11	9.55	13.02
$t_{s_2}$ (min)	7.20	6.57	7.38	8.23	8.52	5.97	5.35	5.3	4.6
$t_{c_{90}}$ (min)	27	28	36	37	39	24	20	21	23
CRI	5.05	4.67	3.49	3.48	3.28	5.55	6.8	6.37	5.4
$\alpha_f$	-	3.93	3.35	3.39	3.23	5.67	6.33	8.79	11.73

temperature range from 50 to 750°C. The average sample mass was about 8 mg.

## RESULTS AND DISCUSSION

### Cure Characteristics

The cure characteristics of unfilled and nano- and micro-silica filled CSM vulcanizates are given in Table II. In order to analyze the cure behavior of samples, the physical and chemical interactions of rubber with filler should be fully studied.<sup>22,23</sup> Two series of data can be extracted from the rheometry test: vulcanization times ( $t_{s_2}$ ,  $t_{c_{90}}$ , CRI) which demonstrate the vulcanization kinetics and the torque values ( $M_L$ ,  $M_H$ ,  $\Delta M$ ) which can be used for interpreting the cross links, whether physical or chemical.

The minimum torque,  $M_L$  can be taken as a measure of the viscosity of the uncured samples. Its value has increased almost in all the samples which confirms the enhancing of the viscosity by increasing the filler loading. This enhancement is attributed to a physical cross-link network. Since the rubber is in its induction period, the chemical cross links have not formed yet. On the other hand, introduction of the filler will hinder the mobility of rubber chains and prevent its deformation and consequently enhance the  $M_L$  value.  $M_L$  can be related to the specific surface area of filler.<sup>24</sup> Increasing the  $M_L$  value indicates that a larger amount of rubber chains have been immobilized on the filler surface thus, reinforcement has occurred. Because the  $M_L$  values for CSM/nano silica is higher than CSM/micro silica composites, it can be concluded that a stronger physical network has formed in the nanocomposites and therefore their reinforcing efficiency is higher.

The maximum torque,  $M_H$  can be taken as the maximum viscosity and stiffness of the fully vulcanized sample and is an approximate measure of the chemical cross link density in the sample.<sup>21</sup> The torque difference ( $M_H - M_L$ ) is directly proportional to the degree of crosslinking of the vulcanizates.<sup>25</sup>

As it is shown in Table II, the maximum torque ( $M_H$ ) and its difference ( $\Delta M = M_H - M_L$ ) increases with the increase of the nano- and micro-silica particles loading. However the higher values are obtained for CSM/nano-silica samples. The higher values of  $M_H$  and  $\Delta M$  for CSM/nano-silica samples can be due to increase in crosslink density which has been also confirmed by swelling test in the next section

The values of the scorch time,  $t_{s_2}$ , optimum cure time,  $t_{c_{90}}$ , and cure rate index, CRI are tabulated in Table II. It is obtained that for composites containing micro silica,  $t_{s_2}$  and  $t_{c_{90}}$  increase monotonously by raising the micro silica loading. Consequently, the CRI which is reverse proportional to the difference of  $t_{c_{90}} - t_{s_2}$ , see eq. (1) decreases. It can be concluded that, introduction and progressive increase in the micro silica loading has extended the vulcanization time and decelerated the rate of vulcanization. This can be explained by the surface chemistry of the micro silica particles which is occupied by acidic hydroxyl, siloxane and silanol groups. These functional are able to adsorb the basic accelerators by the surface hydrogen bonds, deactivate them, and slow down the rate and degree of vulcanization.<sup>26</sup> However for samples containing nano silica another trend has been observed. In CSM/nano-silica samples  $t_{s_2}$  has decreased and CRI increased compared to control sample. These results confirm the acceleration effect upon introduction of nano silica but the question remains is that why micro silica and nano silica act contradictorily while they have similar chemistry surface? This can be explained by the physical network which is proved by the enhancement of  $M_L$ . As mentioned in the first part of this section, the  $M_L$  values have grown in CSM/nano silica compared to CSM/micro silica. Formation of the physical network alters the accessibility of the surface groups so the adsorption of accelerators on the surface of CSM/nano silica is less, compared to CSM/micro silica. Consequently, the inclusion of nano silica speed up the vulcanization and increases the chemical cross link as well.

The higher  $\alpha$ -value for CSM/nano-silica samples indicate a better interfacial interaction between nano-silica particle with the polar rubber as compared to those of CSM/micro-silica samples.<sup>27</sup>

### Swelling Study and Cross-Linking Density Determination

The influence of nano- and micro- silica particles on the time dependent evolution of the swelling of the samples is shown Figure 2(a,b) respectively. In the initial stage the swelling curves exhibit a quasi-linear increase which corresponds to the diffusion controlled mass uptake. This stage is followed by a continuous decrease of the mass uptake rate until a plateau region is reached.<sup>13</sup> The decrease of the plateau values as a function of the nano- and micro-silica loading can be attributed not only to the dilution effect caused by the impenetrable filler but also

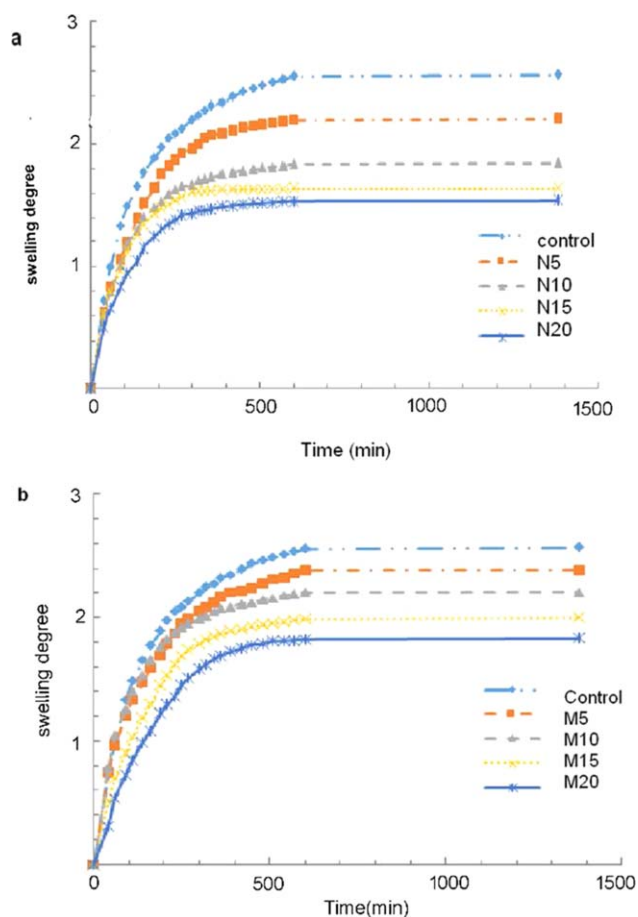


**Figure 2.** Swelling behavior on the time dependent of (a) nano- and (b) micro-silica particle sized filled CSM vulcanizates. [Color figure can be viewed in the online issue, which is available at [wileyonlinelibrary.com](http://wileyonlinelibrary.com).]

to the fact that a physically adsorbed polymer layer is formed on the filler surfaces. The swelling degree decreases and has lower values for CSM/nano-silica samples. This can be explained by linkage formation between polymer chains and functional groups on the silica surface, and by a possible increase in the cross-linking bonds in polymer matrix because of filler influence on the vulcanization reaction.

Table III, represents the cross link density ( $\mu$ ) and volume fraction ( $v$ ) of the nano- and micro-silica particle size filled CSM vulcanizates. The cross-linking density,  $\mu$ , increased with increasing micro- and nano-silica concentrations and was the largest for the sample containing nano-silica particles. As it is known, the lower degree of crosslinking is always accompanied by a higher amount of swelling.<sup>28</sup> The results of the swelling test and cross-linking density measurement seem to agree well

with the results of the cure characteristics and physico-mechanical properties.

The volume fraction of swollen rubber containing micro and nano silica are represented in Table III. It can be seen that incorporation of silica fillers has increased the volume fraction of the rubber samples. Since the rubber chain segments have been adsorbed on the surface of the filler therefore, the fraction of chains which are able to swell, decreases and the volume fraction increases. It is known that nano fillers have higher specific surface area, so interaction area increases and more chain segments become able to be adsorbed on the surface of the filler. Thus, the volume fraction increases compared to the samples containing the micro fillers.

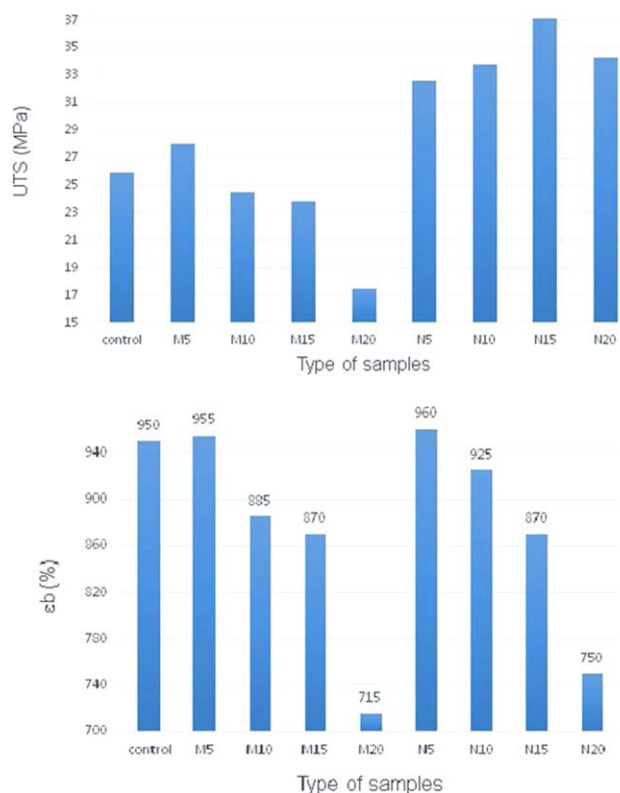
### Mechanical Properties

Figure 3(a,b) compare the tensile strength and elongation at break of the two series of the samples, respectively. Table IV represents the effect of nano- and micro-silica particles loadings (5–20 phr) on modulus, hardness, compression set and abrasion resistance of the samples. It is obvious that, without nano- and micro-silica particles, the unfilled CSM vulcanizates still possesses relatively high tensile strength (25.9 MPa). This is possibly due to the fact that CSM is able to crystallize upon stretching to high tension.<sup>29</sup> It is also observed that with loading of nano-silica particles content at 15 phr and micro-silica particles content at 5 phr tensile strength would increase to 37.1 and 28 MPa respectively. Further increase in nano- and micro-silica particles loading could lead to a significant drop in tensile strength. Thus, at 15 phr nano-silica particles and 5 phr micro-silica particles loading, polymer-filler interaction is maximum whereas at higher filler loading, filler-filler interaction predominates, resulting from agglomeration and a poor dispersion of the filler particles in the filled CSM matrix.<sup>10</sup>

Figure 3(b) shows that by incorporation of 5 phr micro and nano silica to CSM, elongation at break ( $E_b$  %) improves slightly. As it is shown in this Figure, the elongation at break decreases gradually with further increase in micro- and nano-silica loadings. This reduction is due to the stiffening of the matrix both type of filler particles. It is also believed that, the decrease in the molecular mobility is due to the formation of a physical and chemical bonds between the filler particles and the rubber chain segments.<sup>29</sup> The  $E_b$  % values of nano-silica filled compounds are little higher than micro-silica filled compounds as shown in Figure 3(b). This may be because of the higher values of CSM-nano-silica interaction, leading to an increase in the interfacial adhesion between filler and matrix compared to micro-silica filled compounds.

**Table III.** Crosslink Density and Volume Fraction of the Samples

	Sample code								
	Control	M5	M10	M15	M20	N5	N10	N15	N20
Crosslink density ( $\times 10^4$ )	1.46	1.66	1.92	2.28	2.74	1.92	2.64	3.11	3.69
Volume fraction ( $v$ )	0.2198	0.2323	0.2463	0.2641	0.2837	0.2464	0.2797	0.2982	0.3182



**Figure 3.** Comparison of the ultimate tensile strength (UTS) (a) and the elongation at break ( $\epsilon_b$ , %) (b) of the two series of the samples. [Color figure can be viewed in the online issue, which is available at [wileyonlinelibrary.com](http://wileyonlinelibrary.com).]

The M100, M200, and M300 moduli, are also found to increase with increasing micro- and nano-silica loadings, furthermore these values are higher for the nano- than the micro-silica filled samples. Since modulus is a function of crosslink density it could increase with increase in the number of crosslinks.

The hardness of the filled CSM vulcanizates is increased continuously with increasing micro- and nano-silica content and have higher values for CSM/nano-silica samples, which may be attributed to the more stiffening effect.

The increase of hardness, modulus, and tensile strength for nano fillers compared to micro-filled samples may also be explained by the improvement of the degree of adhesion at interfaces between the nano-silica and the CSM rubber matrix.<sup>2</sup>

The compression set of the samples at 5 phr of nano-silica leads to a slight increase, then more increase with the increase of nano-silica content is observed. Whereas at 5 phr of micro-silica an increase is seen and then with more increase of micro-silica content slightly decreased. Comparison of compression set data for the two series of the samples show that, these values are higher for the nano- than the micro- silica filled cross-linked rubbers. This could be attributed to the increase of stiffness and the decrease of the rubber elasticity of the samples.<sup>6</sup> The increase in compression set may also be attributed to the dilution effect.

The abrasion loss of the filled CSM vulcanizates has increased continuously with the increasing of micro- and nano-silica content. In other words, abrasion resistance tends to decrease with increasing the silica content. This could be attributed to the decrement of chain mobility caused by filler incorporation. The CSM chains are flexible so their mobility hinders the abrasion. Incorporation of fillers especially micro fillers, decreases the mobility which is evidenced by increasing the cross link density (see swelling study). The decrement of abrasion resistance is also reported by other researchers.<sup>29</sup>

#### Scanning Electron Microscopy (SEM)

The SEM micrographs of the fracture surface of M5 and M15 cross-linked samples and also N15 and N20 are shown in Figures 4 and 5 respectively. It can be seen that the dispersion of 5 phr of micro-silica particles and 15 phr of nano-silica particles is more uniform in the polymer matrix compared with the other samples, resulting in a higher tensile strength. The samples with higher filler loading doesn't reveal good dispersion in the rubber matrix as a result of the filler agglomeration which is clearly observed from the SEM images of the M10 and N20 cross-linked samples. This is not only attributed to the agglomeration of the particles, but also to the weak interfacial interaction between the filler and the matrix, leading to void formation and therefore deterioration of the samples'

**Table IV.** Mechanical Properties of Unfilled and Nano- and Micro-Silica Particle Sized Filled CSM Vulcanizates

Properties	Control	M5	M10	M15	M20	N5	N10	N15	N20
M100%, MPa	1.11	1.25	1.16	1.27	1.53	1.45	1.8	2.3	3.43
M200%, MPa	1.8	1.95	1.98	2.46	3.09	1.96	2.52	4.3	6.59
M300%, MPa	2.75	3.32	3.3	3.94	4.94	3.15	4.09	7.09	10.49
Hardness (Shore A)	53 ± 0.5	57 ± 1.3	59 ± 0.8	60 ± 1.3	62 ± 0.6	57 ± 1	61 ± 0.4	68 ± 0.4	75 ± 0.7
Compression set, %	37.6 ± 1.6	78.6 ± 1.5	77.2 ± 1.2	73.5 ± 1.4	70.5 ± 1.1	39.4 ± 1.9	73.4 ± 1.6	78.5 ± 0.82	80.6 ± 1.8
Abrasion loss, mm <sup>3</sup>	46 ± 1.5	85 ± 1.4	96 ± 0.9	98 ± 1.3	103 ± 1.5	50 ± 1.3	59 ± 1.2	88 ± 1	85 ± 1.3

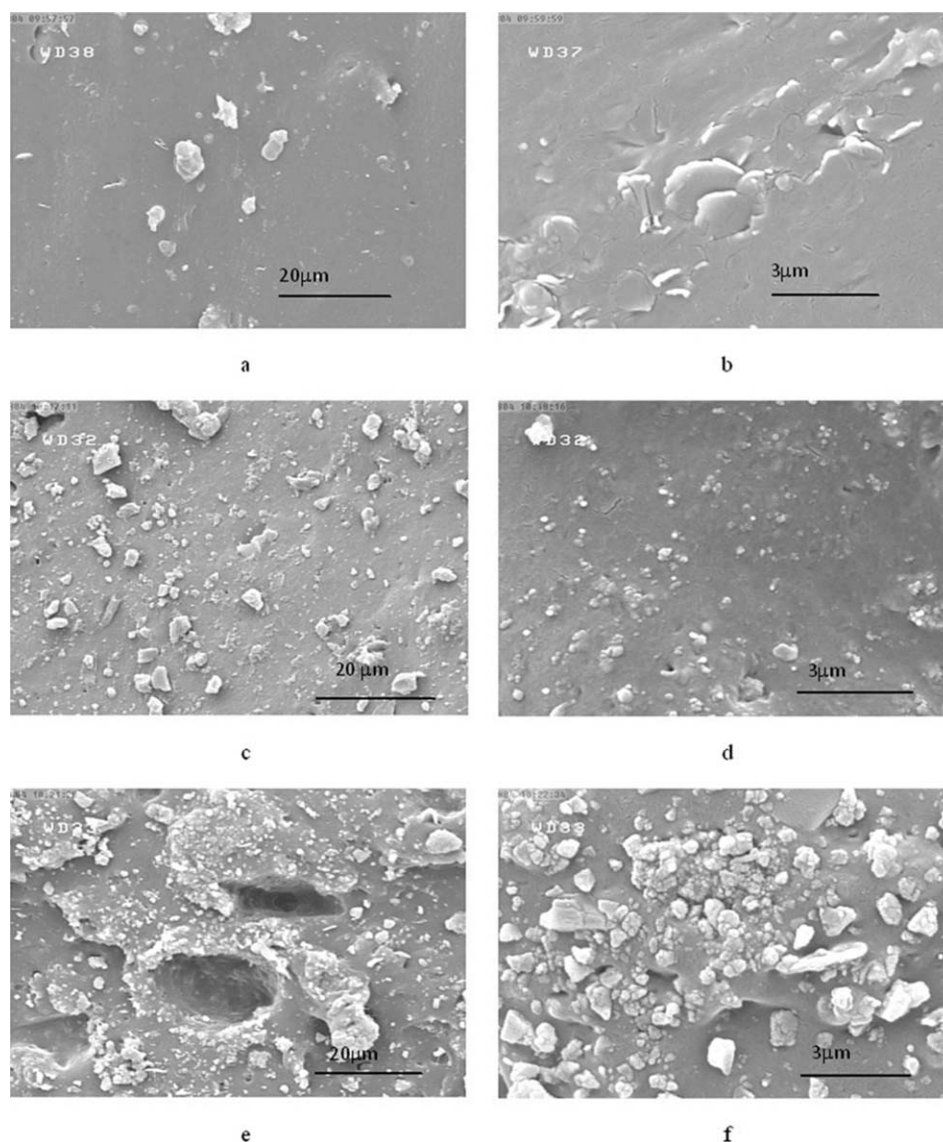


**Figure 4.** SEM micrographs of tensile fractured surface of (a,b) unfilled cross-linked system, (c,d) M5, (e,f) M15.

properties. This observation appears to be in good agreement with the obtained mechanical properties of the samples (see section 3.1).

#### Thermal Analysis

Figure 6 shows the TGA curves of the pure cured CSM and of the filled CSM rubber samples with 5 phr of micro-silica particles and 15 phr of nano-silica particles. These samples were chosen among others because, they revealed the higher mechanical properties. The data extracted from the curves in Figure 6 are presented in Table V.  $T_{5\%}$  and  $T_{10\%}$  show the temperatures at which 5% and 10% of weight loss has occurred respectively. Overall Stabilization Effect (OSE) is a parameter which is gained from TGA curves. This parameter is calculated via integration of the area under  $\Delta\text{mass} \%$  versus temperature curves of Figure 6(b). OSE is a useful parameter which enables us to

have a fair comparison between various samples eq. (5). Positive OSE values mean that the samples are thermally more stable than the virgin polymer while the negative values confirm the desatubilization effect of the filler.<sup>30,31</sup>

$$\text{OSE} = \sum_{T=30}^{800} (\text{mass percent of nanocomposite at } T - \text{mass percent of neat resin at } T) \quad (5)$$

Another parameter which is extracted from TGA data is integral procedure decomposition temperature (IPDT). This value was first introduced by Doyle and is calculated as follows:<sup>32</sup>

$$\text{IPDT} = A * K * (T_f - T_i) + T_i \quad (6)$$

$$A = \frac{s_1 + s_2}{s_1 + s_2 + s_3} \quad (7)$$

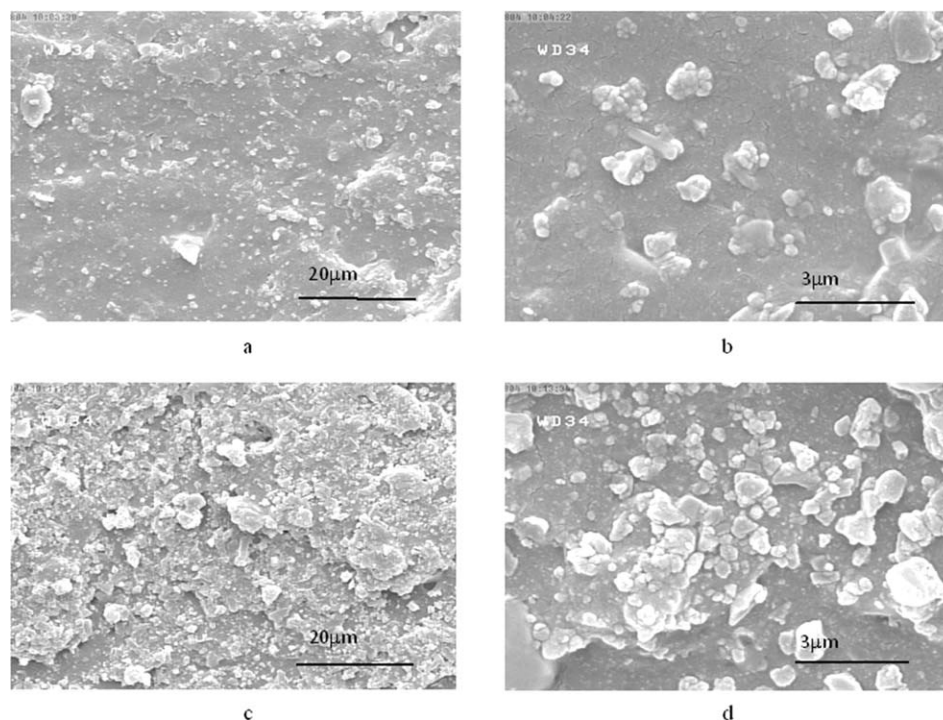


**Figure 5.** SEM micrographs of tensile fractured surface of (a,b) N15 and (c,d) N20 cross-linked samples.

$$K = \frac{s_1 + s_2}{s_1} \quad (8)$$

In this formulas,  $T_i$  is an initial experimental temperature and  $T_f$  is final experimental temperature. The  $S_1$ ,  $S_2$ , and  $S_3$  were depicted by Doyle's proposition in Figure 7.

The thermal decomposition of all the samples occur generally in two main stages: (1) degradation occurs in the temperature region 200–400°C and (2) degradation is about at 470°C. According to the literature, the degradation of the CSM starts with elimination of  $\text{SO}_2\text{Cl}$  groups on the polymer chain and continuous with dehydrochlorination.<sup>33</sup> At higher temperature the backbone of the polymer chain degrades and results in a remainder ash. The data for the initial decomposition temperature (IDT) (3% mass loss), 5 and 10% mass loss temperatures are given in Table V. It can be seen that 3, 5 and 10% mass loss temperatures for 15 phr of nano- and 5 phr of micro-silica filled CSM samples are higher than unfilled compound. Furthermore, 5 and 10% mass loss temperature with 15 phr of nano-silica particles size filled CSM rubber has higher values than other samples, that indicates higher thermal stability of N15 sample can be related to its higher cross-linking density. These results are also in accordance with OSE and IPDT parameters. As it can be seen from Table V, OSE and IPDT for N15 is much higher than M5, so it can be concluded that introduction of 15 phr nano silica had better effect on thermal resistancy, compared to the M5.

It is worth mentioning that, the neat rubber weight of all samples is the same. In other words all samples contain 100 phr neat rubber as mentioned in Table I. TGA data in the Table V

includes the weight difference of the filler considering the higher accuracy, but the impact on the comparison results regarding heat resistance will be negligible small.

#### Effect of Both Micro and Nano Silica

In order to optimize the mechanical properties of CSM composites containing silica, the composites with mixture of fillers (micro and nano) were evaluated. Among various loadings of micro fillers, 5 phr provided the best impact on UTS, EB% and M100%. Consequently, in the hybrid samples, the loading of micro silica was held constant at 5 phr but the nano filler loading varied from 5 to 15 phr. The mechanical properties of the hybrid samples are compiled in Table VI. It can be seen that inclusion of 5 phr nano silica to 5 phr micro silica (M5/N5) has improved UTS dramatically. However further increase in nano silica loading did not increase the UTS remarkably.

By comparing the results (Tables IV and VI), it can be concluded that the N10 and M5/N5 samples have almost the same UTS. However M5/N5 is more preferable compared to N10. Since micro fillers are more popular in industrial applications compared to nano fillers and reducing the amount of nano filler loading will be desirable.

The hardness values of the mixture samples also confirm the superiority of the hybrid samples compared to their micro or nano composite alone. The rubber compounds usually tend to get harder as a result of tensile improvement. The increase of hardness is an imperfection for rubber vulcanizates. Therefore it is desirable to produce compound with high UTS and low hardness. By inclusion of 5 phr nano silica to M5, the desirable properties of N10 will be achieved. Consequently, the M5/N5

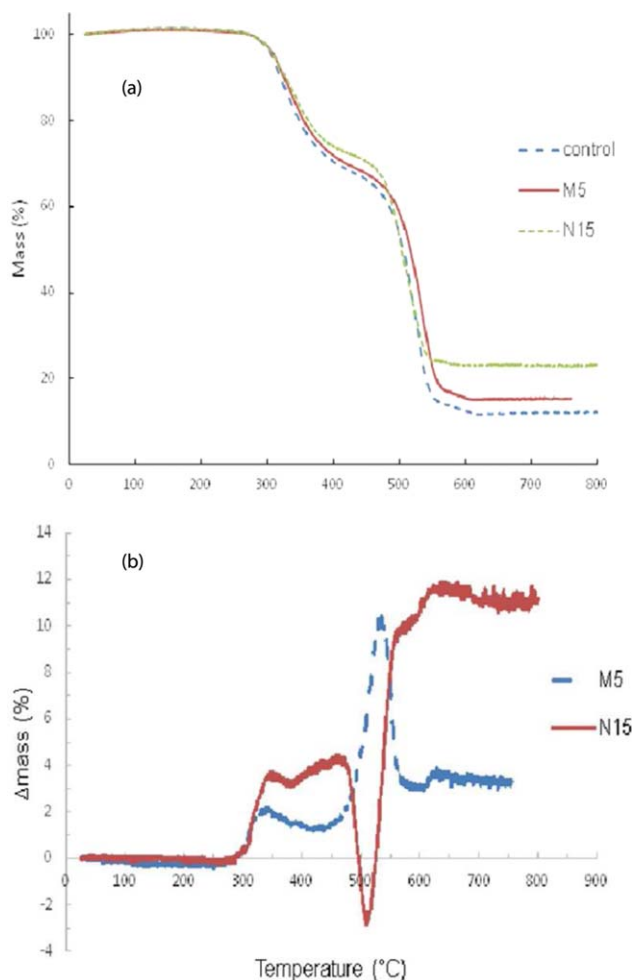


**Figure 6.** TGA curves of unfilled, M5, and N15 cross-linked samples (a), Variation of mass difference between a filled sample and unfilled sample versus temperature (b). [Color figure can be viewed in the online issue, which is available at [wileyonlinelibrary.com](http://wileyonlinelibrary.com).]

sample is the most suitable sample because it is cost-effective and provides superior mechanical properties.

Thermal properties parameters of the M5/N5 are also tabulated in Table VI. The extracted parameters show that M5 and M5/N5 have similar thermal behavior. However it can be claimed that the hybrid sample is more thermally stable compared to M5. Since the OSE and IPDT have raised slightly.

## CONCLUSIONS

In this study, the effect of nano and micro silica particles on cure characteristics, mechanical and thermal properties of CSM

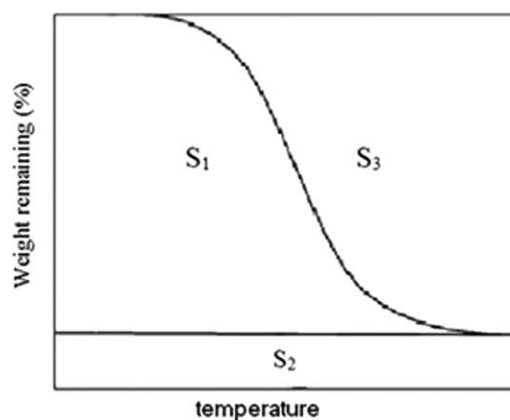


**Figure 7.** Doyle's proposition for calculation of IPDT.

vulcanizates is compared. The vulcanization characteristics and swelling behavior of filled /CSM samples mainly depends on the filler concentration and their specific surface area. Incorporation of micro silica decelerated the vulcanization and raised the cross link density. While the nano silica particles had an acceleration effect on vulcanization. Their impact on the cross link density was also stronger compared to micro silica. These differences are attributed to different physical interaction which is a result of different specific surface area. In the case of micro silica, the curing system is adsorbed on the surface of filler but in the CSM/nano silica composites, a physical network is formed which provide reinforcing efficiency and accelerates the vulcanization as well. Because of that, the nano composites revealed superior mechanical properties.

Tensile strength, elongation at break, compression set, hardness, and abrasion resistance of the prepared samples have been studied. Ultimate tensile strength increases with increasing in both of the fillers loading up to 15 phr nano- silica and 5 phr micro-silica in the filled CSM vulcanizates. At higher fillers loading, tensile strength is decreased, resulting from a non-uniform dispersion of the nano- and micro- silica in the filled CSM rubbers. Abrasion resistance gradually decreased with increase in modulus of the samples and thus, reducing the elasticity of the vulcanizates. The nano-silica filled samples have higher values for mechanical properties than micro-silica particle sized filled rubbers. This would be as a result of greater contact area of the nano-filler, greater adsorption of the polymer chains by the surfaces of nano silica particles and the improvement of the degree of adhesion at interfaces between the nano-silica and the CSM rubber. Scanning electron microscopy on fracture surfaces of the tensile specimens shows a more homogenous phase dispersion and strong filler–matrix interaction, resulting in a

**Table V.** TGA Data of the Selected Samples

Sample	$T_{3\%}, ^\circ\text{C}$	$T_{5\%}, ^\circ\text{C}$	$T_{10\%}, ^\circ\text{C}$	Remainder, wt %	$T_i$	$T_f$	IPDT	OSE
Control	404.6	307.7	320.5	12	–	–	–	–
N15	455	310.22	328.2	23.3	24.5	800	1051	2973
M5	420.4	311.6	326	15.5	760	24.5	654	1437

**Table VI.** Mechanical and Thermal Properties of Hybrid Samples

Properties	Control	MS	M5/N5	M5/N10	M5/N15
UTS (MPa)	25.9 ± 1.5	28 ± 0.9	33 ± 1.4	31 ± 1.1	32 ± 0.87
EB (%)	950	955	960	955	900
M100%, MPa	1.11	1.25	1.4	1.6	2.3
M200%, MPa	1.8	1.95	2.74	3.1	4.78
M300%, MPa	2.75	3.32	4.49	5.25	7.71
Hardness (Shore A)	53 ± 0.5	57 ± 1.3	60 ± 0.9	63 ± 0.64	69 ± 1
T <sub>3%</sub>	404.6	420.4	302.7	-	-
T <sub>5%</sub>	307.7	311.6	311.6	-	-
T <sub>10%</sub>	320.5	326	326	-	-
IPDT	-	654	655.4	-	-
OSE	-	1437	1583	-	-

higher tensile strength for the M5 and N15 samples compared to the other samples. The thermogravimetric analysis indicates that thermal stability of the samples with 5 phr of micro-silica particles and 15 phr of nano-silica particles are better than that of pure CSM and is higher for the samples containing 15 phr of nano-silica particles.

To benefit both micro and nano silica, hybrid samples were studied. The results confirmed that the compound containing 5 phr nano silica and 5 phr micro silica (M5/N5) is a suitable sample because of its superior mechanical and thermal properties.

## REFERENCES

- Kantala, C.; Wimolmala, E.; Sirisinha, C.; Sombatsompop, N. *Polym. Adv. Technol.* **2009**, *20*, 448.
- Markovic, G.; Samaržija-Jovanovic, S.; Jovanovic, V.; Marinovic, M.; Cincovic, M. *J. Therm. Anal. Calorim.* **2010**, *100*, 881.
- Sae-oui, P.; Sirisinha, C.; Wantana, T.; Hatthapanit, K. *J. Appl. Polym. Sci.* **2007**, *104*, 3478.
- Liu, X.; Zhao, S. *J. Appl. Polym. Sci.* **2008**, *108*, 3038.
- Bazgir, S.; Katbab, A. A.; Nazockdast, H. *J. Appl. Polym. Sci.* **2004**, *92*, 2000.
- Sae-oui, P.; Sirisinha, C.; Thepsuwan, U.; Hatthapanit, K. *Eur. Polym. J.* **2007**, *43*, 185.
- Arayaprane, W.; Rempel, G. L. *J. Appl. Polym. Sci.* **2008**, *110*, 1165.
- Pal, K.; Rajasekar, R.; Jin Kang, D.; Xiu Zhang, Z.; Pal, S. K.; Das, C. K.; Kuk Kim, J. *Mat. Des.* **2010**, *31*, 677.
- Gu, Z.; Song, G.; Liu, W.; Gao, J.; Dou, W.; Lu, P. *J. Appl. Polym. Sci.* **2010**, *115*, 3365.
- Nanda, M.; Tripathy, D. K. *Exp. Polym. Lett.* **2008**, *2*, 855.
- Roychoudhury, A. *Rubber Chem. Technol.* **1995**, *68*, 815.
- Das, A.; Debnath, S. C.; De, D.; Basu, D. K. *J. Appl. Polym. Sci.* **2004**, *93*, 196.
- Sahoo, N. G.; Shiva Kumar, E.; Das, C. K.; Panda, A. B.; Pramanik, P. *Macromol. Res.* **2003**, *11*, 506.
- Bai, X.; He, X.; Zhang, J.; Zhu, X.; Zhang, H.; Cheng, R.; Liu, B. *Polym. Compos.* **2012**, *33*, 940.
- Markovic, G.; Marinovic-Cincovic, M.; Jovanovic, V.; Samaržija-Jovanovic, S.; Budinski-Simendic, J. *Compos. Part B* **2013**, *55*, 368.
- Markovic, G.; Veljkovic, O.; Marinovic-Cincovic, M.; Jovanovic, V.; Samaržija-Jovanovic, S.; Budinski-Simendic, J. *Compos. Part B* **2013**, *45*, 178.
- Nanda, M.; Tripathy, D. K. *J. Appl. Polym. Sci.* **2012**, *126*, 46.
- Liu, X.; Zhao, S. *J. Appl. Polym. Sci.* **2008**, *108*, 3038.
- Markovic, G.; Devic, S.; Marinovic-Cincovic, M.; Budinski-Simendic, J. *KGK. Kautschuk, Gummi, Kunststoffe* **2009**, *62*, 299.
- Wilson, K. V.; Smith, B.; Macdonald, J. M.; Schoonover, J. R.; Castro, J. M.; Smith, M. E.; Cournoyer, M. E.; Marx, R.; Steckle, W. P. *Polym. Degrad. Stab.* **2004**, *84*, 439.
- Markovic, G.; Radovanovic, B.; Marinovic, M.; Budinski, J. *Mater. Manuf. Process* **2009**, *24*, 1224.
- Pourhossaini, M. R.; Razzaghi-Kashani, M. *Polymer* **2014**, *55*, 2279.
- Hosseini, S. M.; Razzaghi-Kashani, M. *Polymer* **2014**, *55*, 6426.
- Li, Z. H.; Zhang, J.; Chen, S. J. *Expr. Polym. Lett.* **2008**, *2*, 695.
- Markovic, G.; Samaržija-Jovanovic, S.; Jovanovic, V.; Marinovic, M.; Cincovic, J. *Therm. Anal. Calorim.* **2010**, *100*, 881.
- Ansarifard, M. A.; Chugh, J. P.; Haghghat, S. *Iran. Polym. J.* **2000**, *9*, 81.
- Sae-oui, P.; Sirisinha, C.; Wantana, T.; Hatthapanit, K. *J. Appl. Polym. Sci.* **2007**, *104*, 3478.

28. Klingender, R. C. *Handbook of Specialty Elastomers*; Taylor & Francis Inc: New York, **2008**; Chapter 9, p 301.
29. Rattanasom, N.; Saowapark; Deeprasertkul, C. *Polym. Test* **2007**, *26*, 369.
30. Hesami, M.; Bagheri, R.; Masoomi, M. *J. Appl. Polym. Sci.* **2014**, *131*, 1.
31. Hesami, M.; Bagheri, R.; Masoomi, M. *Iran. Polym. J.* **2014**, *23*, 469.
32. Doyle, C. D. *Anal. Chem.* **1961**, *33*, 77.
33. Minsker, K. S.; Steklova, M. A.; Zaikov, G. E. *Polym. Degrad. Stab.* **1990**, *28*, 227.